35th Annual International Conference of the IEEE EMBS
Osaka, Japan, 3 - 7 July, 2013

Coupling Invariant Inductive Link for Wireless Power Delivery to a Retinal Prosthesis

David C. Ng, *Member, IEEE* and Efstratios Skafidas, *Senior Member, IEEE*

Abstract— **Inductive links are used in various applications to transfer power and data wirelessly. To achieve optimal performance in terms of voltage gain and maximum power transfer, these links are often operated at high coupling regime or under resonant frequency condition. However, these conditions may vary due to variations in the link itself or load. As a result, the link performance drops and the design of driving circuit become more complicated in order to compensate for the reduction in performance. In this work, we investigate an inductive link that has constant coupling. The tradeoff for invariant coupling is a reduction in coupling coefficient. In this study, we found that a reduction of 66 % exist between the traditional inductive link and our design. However, the advantage of coupling invariance outweighs the negative effect of large coil separation and varying conditions of a traditional one-pair coil link. The new link has the potential for powering a retinal implant.**

I. Introduction

Inductive links are adopted in many fields from electrical to biomedical engineering for transferring power and data without the need for wires. Examples include wireless charging of portable devices, medical implants, and chip-to-chip communication [1]–[3].

The simplest inductive link consists of a pair of inductive coils that are physically separated. As a general rule, smaller and more widely separated coils transfer less power than do bigger and closely spaced coils. The principle of operation of the link involves the generation of magnetic field by moving electrical charges in one of the coil. This magnetic field induces an electromotive force (EMF) when a second coil is placed close to it. Hence, by connecting an electrical energy source to the first coil and a load to the second coil, energy can be transmitted wirelessly through the inductive link to power the load.

There are many factors that dictate the effectiveness of the coils in transferring power. Among the major factors are impedance and inductance of the coils [4], relative orientation of the coils [5], and electromagnetic property of the media surrounding the coils [6]. One often overlooked factor is the frequency of operation and the natural resonance frequency of the link. Because the factors mentioned are functions of frequency, the choice of frequency and the tradeoffs due to that choice are very important aspects in the operation of the link.

Apart from that, inductive links operate in the near field regime as opposed to far field regime operation for radio frequency transceivers. An inductive link is not designed to work as a far field transmitter, however, the choice of operation frequency should be such that electromagnetic interference (EMI) with surrounding devices are avoided. This adds another constraint to the design of the link.

Furthermore, operation in media such as air or biological tissue and fluid is not uncommon for many biomedical applications. An example is the use of inductive link for powering a retinal implant. In this case, apart from the constantly varying load, the link has to contend with constant motion of the implant. This presents challenges in achieving optimal energy transfer as the driver circuitry becomes more complicated.

In the past, we have made qualitative investigation on using two-pair coil inductive link for transferring power to a retinal implant [7]. The motivation of the work is to render the link immune to relative motion and changes in orientation of the coils. In this work, we present a more quantitative approach in characterizing the link.

II. Model Analysis

A. Physical System

Coils used in inductive links should ideally have no resistance or capacitance. Real coils however, have both the former and latter. These coils can be modeled using circuit elements [8]. The simplest model consists of a resistor in series with an inductor. This model is adequate when the operation frequency is low compared to the natural resonant frequency of the coil. The resonant frequency of the coil can also be tuned by introducing a capacitor. This allows the circuit to be operated at resonance, usually at a lower frequency, which brings about the advantage of voltage gain as well as increase in apparent coupling. As mentioned earlier, when operated at frequencies well below the natural resonant frequency, the coil impedance can be modeled with sufficient accuracy with

$$Z = R + jX. \tag{1}$$

National Information and Communication Technologies Australia (NICTA) is supported by the Australian Government as represented by the Department of Broadband, Communications and the Digital Economy, and the Australian Research Council through its Information and Communication Technologies Centre of Excellence program.

D. C. Ng is with the National Information and Communications Technologies Australia (NICTA), Victoria Research Laboratory (VRL), Melbourne, VIC 3010 Australia (tel: +61-3-9035-3657; e-mail: david.ng@nicta.com.au).

E. Skafidas is with the University of Melbourne, Melbourne, VIC 3010 Australia (e-mail: sskaf@unimelb.edu.au).

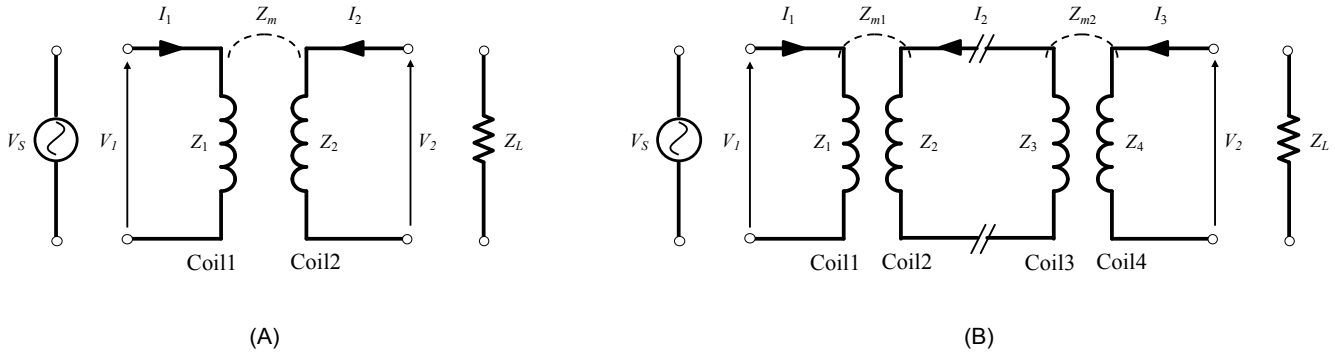

Figure 1. Circuit schematic for; (A) one-pair and (B) two-pair coil inductive link.

The following matrix equation describes the circuit characteristic of the inductive link as shown in Fig. 1 (A)

$$\begin{bmatrix} V_1 \\ V_2 \end{bmatrix} = \begin{bmatrix} Z_1 & Z_m \\ Z_m & Z_2 \end{bmatrix} \begin{bmatrix} I_1 \\ I_2 \end{bmatrix}, \tag{2}$$

where Z_1, Z_2 and Z_m are the impedance of the left coil, right coil and the coupling impedance, respectively. By considering Kirchoff's voltage law (KVL) for both the left hand side (LHS) and right hand side (RHS) of the link when a voltage source and load are connected as shown in Fig. 1, we obtain the following equations

$$I_2 = I_1 \frac{Z_m}{Z_2 + Z_L}, \tag{3}$$

and

$$V_S = I_1 \left(Z_1 - \frac{Z_m^2}{Z_2 + Z_L} \right). \tag{4}$$

We have assumed that the induced voltage $V_m = I_1 Z_m$ is present on the RHS. From (4), the impedance as seen by the voltage source is given by the ratio of V_s and I_1 which is

$$Z = Z_1 - \frac{Z_m^2}{Z_2 + Z_L}. \tag{5}$$

Resonance condition of the loaded link can be obtained when the imaginary component of this impedance equates to zero. In other words, the resonant frequency ω_0 can be obtained when solving the equation $\Im\{Z\} = 0$. From (5), it is apparent that the resonance frequency is a strong function of the coupling impedance and the load. The resonant frequencies for the unloaded link are simply self-resonance frequencies of the respective coils which are independent of each other. Another important measure of the link performance is the coupling coefficient. It is defined as

$$k = \frac{M}{\sqrt{L_1 L_2}}, \tag{6}$$

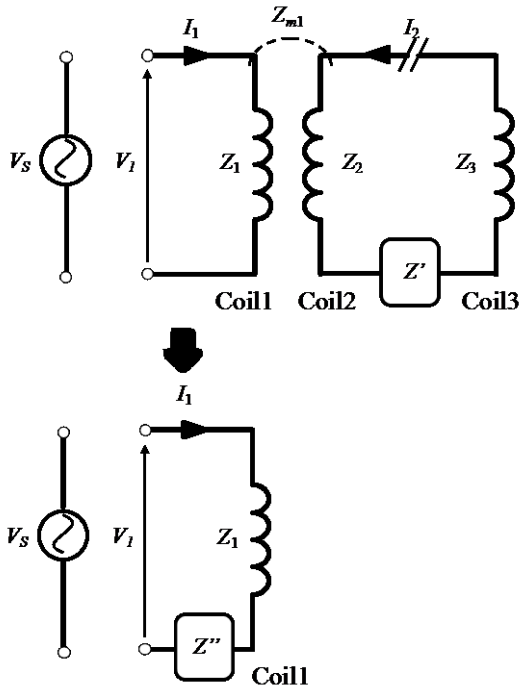

Figure 2. Progressive reduction of two-pair two-port coil inductive link to a single port two-terminal circuit.

where L_1, L_1 and M are the inductance of the left coil, right coil and the mutual inductance of the link, respectively.

B. Characterization

A useful method to characterize inductive link is by considering it as a two-port network. Using a network analyzer, one can very quickly determine its characteristic represented by S-parameters [9]. S-parameter measurement is easy because measuring voltage across the ports is relatively easy compared to accurate current measurement. The following matrix equation describes a two-port network;

$$\begin{bmatrix} V_1^- \\ V_1^+ \end{bmatrix} = \begin{bmatrix} S_{11} & S_{12} \\ S_{21} & S_{22} \end{bmatrix} \begin{bmatrix} V_2^- \\ V_2^+ \end{bmatrix}. \tag{7}$$

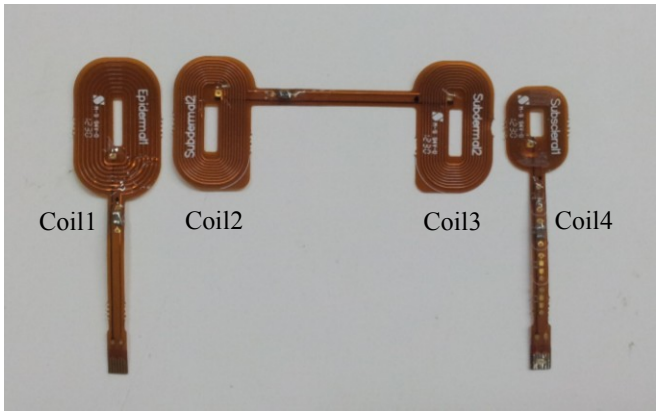

Figure 3. Two-pair coils fabricated using flexible printed circuit technology.

Once, the S-parameters of the network is obtained, it is easy to convert the S-parameters into Z-parameters which can then be used in the matrix of (2).

The coupling coefficient of the link can be evaluated using the following equation;

$$k = \frac{\Im(Z_{12})}{\sqrt{\Im(Z_{11})\Im(Z_{22})}}. \tag{8}$$

This is the apparent coupling coefficient. When the measurement frequency is less than the resonant frequency, The value k from (8) will approach the value given by (6).

III. Two-pair Coil Inductive Link

We can make an inductive link insusceptible to changes in coupling by introducing an additional pair of coils configured as shown in Fig. 1 (B). When the separation between adjacent coils; Coil1-Coil2 and Coil3-Coil4 are kept constant, it allows the magnetic flux across the links to remain constant even though there is relative motion between Coil1 and Coil4.

If we look at the terms in (5), the first term is the uncoupled Coil1 impedance while the second term is the reflected impedance from Coil2 and load. Based on this observation, the two-pair coil link can be progressively reduced to a 1-port circuit as shown in Fig. 3. The impedance as seen by the source for the unloaded case is

$$Z = Z_1 - \frac{Z_{m1}^2}{\underbrace{Z_2 + Z_3}_{Z'}}, \tag{9}$$

For the loaded case, the impedance is

$$Z = Z_1 - \frac{Z_{m1}^2}{\underbrace{Z_2 + Z_3 - \frac{Z_{m2}^2}{Z_4 + Z_L}}_{Z''}}, \tag{10}$$

TABLE I. Coil Dimension and Parameter

Dimension and Parameter	Coils		
	Coil 1	*Coil 2/Coil 3*	*Coil 4*
Width [mm]	13.6	11.6	9.3
Height [mm]	23.2	21.8	13.6
Spiral turns	8	8	14
Track spacing [mm]	0.1	0.254	0.254
Track width [mm]	0.1	0.254	0.254
Resistance [Ω]	1.00	-	3.00
Inductance [μH]	1.00		2.15

Here, as with (5), if the link impedance Z_{m1} and Z_{m2} can be kept constant, the impedance seen by the driver will be invariant. This relaxes the requirement for the design of the driver circuit. The coupling coefficients for the link exist between Coil1 and Coil2, Coil3 and Coil4 and Coil1 and Coil4.

IV. Method and Result

A. Experiment

The coil form factor as shown in Fig. 3 was iteratively designed through consultation with ophthalmologists for ease of surgical insertion into a patient yet is able to provide a large enough area for efficient power transmission. In the final product, the materials used will be based on approved biocompatible material. For quick prototyping, flexible printed circuit technology is used [10]. These coils are rectangular in shape with conductive tracks starting from the outer dimension spiraling to the inside. Coil1 which is placed on the skin is largest. This is followed by Coil2 which is to be placed adjacent to Coil1 under the skin. Coil3 which is electrical connected to Coil2 have the same dimension and parameter. Coil3 is to be placed on the eyeball while Coil4 which has to be inserted under the sclera is smallest. The tracks on the coils have fixed width and spacing in between turns. The dimension and parameters of the coils are listed in Table 1.

An Agilent E5071C vector network analyzer was used to obtain S-parameter measurements. Frequency was swept from 9 kHz to 100 MHz. A custom made jig was used to vary coil separation with accuracy of 1 mm resolution. The performance of the two-pair coil link was compared to a one-pair coil by comparing coupling coefficient. For the one-pair coil case, the coils were placed facing each other and separation was increased from 0 mm to more than 40 mm. For the two-pair coil case, the separation between adjacent pair of coils was toggled between 0 mm and 1 mm, thus giving four possible combinations. This replicates the range of conditions when the coils are deployed on a patient.

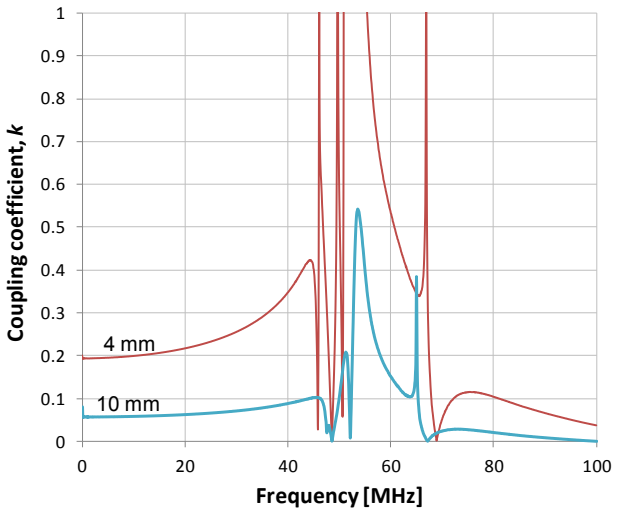

Figure 4. Measured coupling coefficient of one-pair coil as a function of frequency for two separations; 4 mm and 10 mm only (other plots are omitted for clarity).

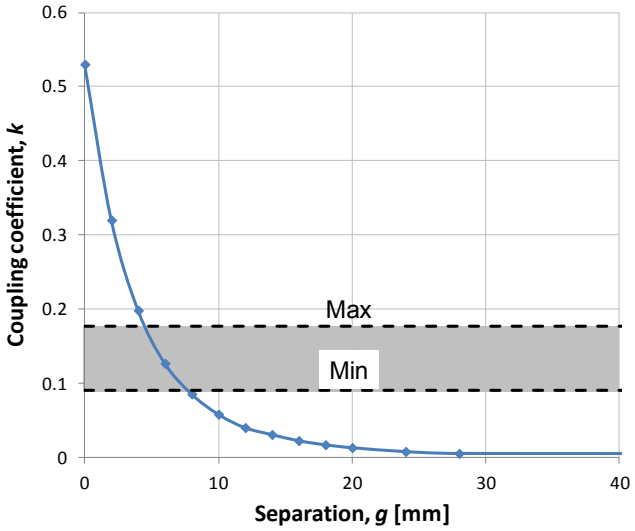

Figure 5. Comparison between coupling coefficient at 10 MHz for one-pair (line) and two-pair (shaded) coils. Max correspond to 0 mm separation between Coil1 and Coil2, and Coil3 and Coil4 while Min correspond to 1 mm separation for the above mentioned coils.

B. Result

Fig. 4 shows the measured coupling coefficient k as a function of frequency based on (7). It can be seen that k is constant at lower frequencies and starts to increase as the frequency approaches the resonant frequency of the coils. There are regions where k approaches unity. This is due to the effect of resonance where there is a crossover of impedance from being inductive to capacitive. By connecting a tuning capacitor to the coil, we can tune the link operation frequency to coincide with large apparent k values.

Coupling coefficient values was extracted from measurement data at 10 MHz and plotted against coil separation as shown in Fig. 5. The maximum coupling coefficient corresponding to zero coil separation for the one-pair coil and two-pair coil is 0.53 and 0.18, respectively. This represents a reduction of about 66 %. In actual operating condition, however, the separation between the coils for the one-pair link would be larger due to the fact that Coil1 would be external to the patient and Coil2 would be closer to the implant inside the eye. For one-pair coil separation beyond 7 mm, its coupling coefficient is lower compared to the minimum value for the two-pair coil link.

V. Conclusion

We have shown that the two-pair coil link is able to keep coupling coefficient constant even with relative motion between coils. Compared to a one-pair coil link which requires large separation gap and has to contend with constant relative motion between the coils when implemented on a retinal prosthesis, the two-pair coil offer clear advantage.

Acknowledgment

The authors acknowledge the helpful discussion with Mark Halpern on inductive links. We would also like to thank Nick Opie and Wilson Heriot for useful discussion regarding coil dimensions.

References

[1] J. Hirai, T. Kim, A. Kawamura, and S. Member, "Study on intelligent battery charging using inductive transmission of power and information," *IEEE Trans. Power Electronics*, vol. 15, no. 2, pp. 335–345, Mar. 2000.

[2] M. Ghovanloo and K. Najafi, "A wireless implantable multichannel microstimulating system-on-a-chip with modular architecture," *IEEE Trans. Neural Syst. Rehabi. Eng.*, vol. 15, no. 3, pp. 449–457, Sep. 2007.

[3] N. Miura, D. Mizoguchi, M. Inoue, T. Sakurai, and T. Kuroda, "A 195-Gb/s 1.2-W inductive inter-chip wireless superconnect with transmit power control scheme for 3-D-stacked system in a package," *IEEE J. Solid-State Circuits*, vol. 41, no. 1, pp. 23–34, Jan. 2006.

[4] R. Rodriguez, J. Dishman, F. Dickens, and E. Whelan, "Modeling of two-dimensional spiral inductors," *IEEE Transactions on Components, Hybrids, and Manufacturing Technology*, vol. 3, no. 4, pp. 535–541, Dec. 1980.

[5] M. Soma, D. C. Galbraith, and R. W. White, "Radio-frequency coils in implantable devices: misalignment analysis and design procedure," *IEEE Trans. Biomed. Eng.*, vol. BME-34, no. 4, pp. 276–282, Apr. 1987.

[6] B. Noureddine, M. Mohamed, and K. Smain, "Attenuation in Transferred RF Power to a Biomedical Implant due to the Absorption of Biological Tissue," in *Proc. World Academy of Science, Engineering and Technology*, vol. 10, pp. 165–168, Dec. 2005.

[7] D. C. Ng, C. E. Williams, P. J. Allen, S. Bai, C. S. Boyd, H. Meffin, M. E. Halpern, and E. Skafidas, "Wireless power delivery for retinal prostheses," in *Proc. IEEE Engineering in Medicine and Biology Society Conf.*, Aug. 30-Sep. 3 2011, pp. 8356–60.

[8] N. M. Nguyen and R. G. Meyer, "Si IC-compatible inductors and LC passive filters," *IEEE J. Solid-State Circuits*, vol. 25, no. 4, pp. 1028–1031, Aug. 1990.

[9] D. M. Pozar, *Microwave Engineering*, 4th ed., Hoboken, NJ: Wiley, 2012, pp. 165–194.

[10] U.-M. Jow and M. Ghovanloo, "Design and Optimization of Printed Spiral Coils for Efficient Transcutaneous Inductive Power Transmission," *IEEE Trans. Biomedical Circuits and Systems*, vol. 1, no. 3, pp. 193–202, Sep. 2007.